

## PLASMA-ASSISTED FABRICATION OF POROUS HETEROGENEOUS METAL/METAL OXIDE COATINGS

Max PAVLOVIĆ<sup>1</sup>, Jan HANUŠ<sup>1</sup>, Marek PROCHÁZKA<sup>2</sup>, Ondřej KYLIÁN<sup>1</sup>

<sup>1</sup>Charles University, Faculty of Mathematics and Physics, Department of Macromolecular Physics, Prague 8, Czech Republic, EU, [ondrej.kylian@matfyz.cuni.cz](mailto:ondrej.kylian@matfyz.cuni.cz)

<sup>2</sup>Charles University, Faculty of Mathematics and Physics, Institute of Physics, Prague 2, Czech Republic, EU

<https://doi.org/10.37904/nanocon.2025.5169>

### Abstract

Porous nanomaterials are essential for a wide range of modern technologies due to their high specific surface area. While single-material systems have been extensively studied in the past decades, bi-material nanostructures are nowadays attracting increasing interest, as these materials may offer improved performance, new functionality or just combine two functionalities in one platform. This work introduces and investigates a novel strategy for the solvent-free synthesis of two-component transition metal-oxide/metal (TMeO/Me) nanoparticle-based coatings, which combines a magnetron-based gas aggregation source for nanoparticle synthesis with conventional magnetron sputtering. As shown in an example of Ta<sub>2</sub>O<sub>5</sub>/Au, depending on the deposition procedure used, the coatings with different architectures may be produced in this way.

**Keywords:** Nanoparticles, gas aggregation sources, bi-component porous coatings

### 1. INTRODUCTION

Transition metal oxide/metal (TMeO/Me) nanocomposites constitute an increasingly demanded class of functional nanomaterials across diverse technological fields. The popularity of these heterogeneous systems is primarily connected with their unique properties. First, the inherent dual-functionality allows for the integration of distinct properties within a single platform. An example is the development of UV-light-recyclable Surface-Enhanced Raman Spectroscopy (SERS) platforms, where the plasmonic metal provides signal enhancement, and the semiconducting TMeO facilitates UV-induced photo-catalytic self-cleaning [1-3]. Second, the interfacial coupling can significantly boost a singular property. An example of this is the dramatic enhancement of SERS activity beyond the capabilities of the isolated TMeO or plasmonic components reported recently for V<sub>2</sub>O<sub>5</sub>/Au [4]. Third, the heterostructures can enable entirely new phenomena, such as, for instance, Photo-Induced Enhanced Raman Spectroscopy (PIERS) [5-7]. This technique exploits the light-activated charge-transfer mechanism between metal, TMeO and analyte, leading to an extraordinary enhancement of the Raman signal.

Achieving these desired functional properties is critically dependent on the precise control over the size, morphology, and three-dimensional architecture of the TMeO/Me system. Consequently, the development of synthetic methods that provide high control over the properties of produced nanomaterials remains an active area of research. Herein, we introduce a versatile, solvent- and linker-free approach combining the gas aggregation sources of nanoparticles (NPs) with sputter-deposition of the metal component. We systematically investigate three distinct fabrication strategies with an emphasis on the resulting architectural control within the porous coatings. The Ta<sub>2</sub>O<sub>5</sub>/Au system is employed as a model platform to demonstrate the applicability of these methodologies.

## 2. EXPERIMENTAL

### 2.1 Deposition procedure

Ta nanoparticles were produced by a home-built, magnetron-based gas aggregation chamber of Haberland construction [8]. It consisted of a 3-inch magnetron with a 3 mm thick Ta target (Kurt J. Lessker), which was introduced to a water-cooled, stainless-steel aggregation chamber with an inner diameter of 100 mm (**Figure 1**) and powered by a DC power source (Advanced Energy). The aggregation chamber was equipped with a pressure gauge (MKS) and mass flow controller (MKS) to introduce the working gas (Argon in this study) and ended with a conical lid with a focusing orifice (20 mm long and 3.5 mm in diameter). The aggregation chamber was attached to the main, high-vacuum deposition, which was pumped by a scroll (Edwards) and turbomolecular (Pfeiffer) pumps. The deposition of Ta NPs was done at a gas flow of 6 sccm with a corresponding pressure in the aggregation chamber of 82 Pa. The magnetron was operated at constant current mode with a current of 300 mA. These operational conditions were selected based on preliminary tests. These showed that the selected conditions allow the production of Ta NPs at a rate close to 2 mg/hour.

Finally, to transform Ta NPs to Ta<sub>2</sub>O<sub>5</sub> ones, the NPs were annealed in open air using an Ohaus Guardian hot plate. The annealing was performed at a temperature of 500 °C for 30 minutes.

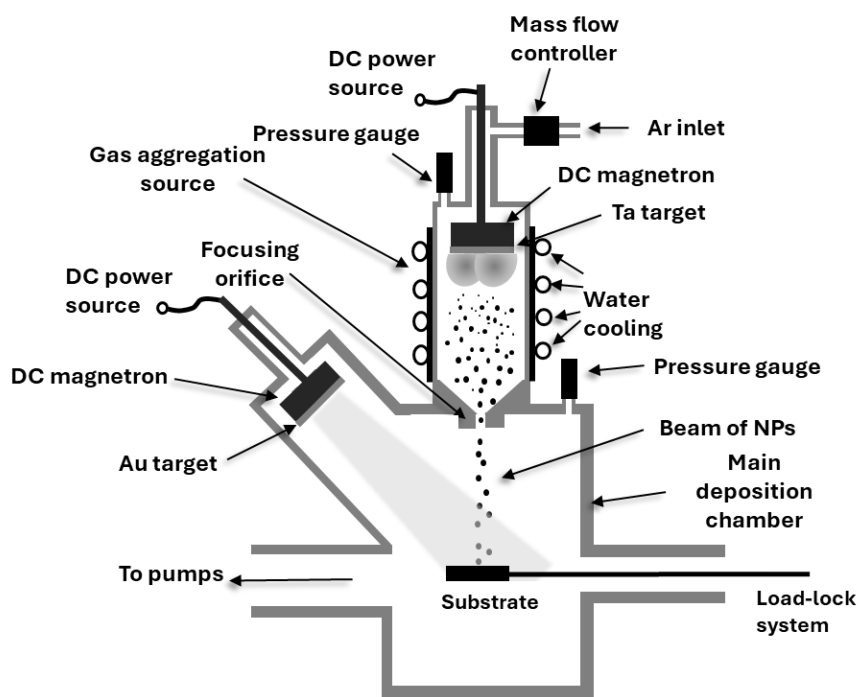


**Figure 1** Deposition set-up

To produce bi-component porous coatings, the main deposition chamber was also equipped with an auxiliary 2-inch magnetron with an Au target (Safina, purity 99.99%). The Au sputtering was performed in a constant current mode of the DC power supply (Advanced energy) at the pressure in the main deposition chamber of 3 Pa and magnetron currents up to 100 mA.

### 2.2 Samples characterisation

The morphology of the produced coatings was analysed by scanning electron microscopy (SEM). The SEM measurements were performed using a field-emission microscope (JEOL) operated in both secondary (SE) and back-scattered electron (BSE) modes (working distance of 10 mm, accelerating voltage of 15 kV). The elemental composition of the samples was evaluated using the energy-dispersive X-ray spectroscopy (EDX)

by means of a JEOL detector attached to the SEM. A working distance during the EDX measurements was 10 mm, and the measurements were performed at an accelerating voltage of 15 kV and a probe current of 7.475 nA. In addition to EDX, the chemical structure of the surfaces of the samples was determined by X-ray Photoelectron Spectroscopy (XPS). The XPS spectra were acquired by means of an XPS spectrometer equipped with a hemispherical analyser (Phoibos 100, Specs) and an Al K $\alpha$  X-rays source (1486.6 eV, 200 W, Specs) at a constant take-off angle of 90°. The XPS spectra were subsequently processed by CASA XPS software.

### 3. RESULTS AND DISCUSSION

#### 3.1 Synthesis of Ta<sub>2</sub>O<sub>5</sub> nanoparticles

The first step of this investigation focused on the controlled deposition and subsequent characterisation of Ta NPs. SEM analysis (**Figure 2a**) revealed a film morphology consisting of uniform, near-spherical nanoparticles exhibiting a narrow size distribution. According to the statistical evaluation, the mean size of as-deposited NPs is  $19 \pm 2$  nm. Furthermore, the high-resolution XPS of the Ta 4f core-level spectrum (**Figure 2b**) confirmed the presence of mixed chemical states. The XPS spectrum exhibited a doublet characteristic of metallic Ta (Ta<sup>0</sup>) at binding energies of 21.8 eV and 23.6 eV, coexisting with a second doublet at 26.3 eV and 28.2 eV. This higher-energy doublet is typically assigned to the Ta<sup>5+</sup> chemical state, i.e., corresponds to Ta<sub>2</sub>O<sub>5</sub> [9]. Despite the oxygen-free deposition environment, the existence of Ta<sub>2</sub>O<sub>5</sub> is attributed to the rapid surface oxidation of Ta upon its exposure to ambient air.

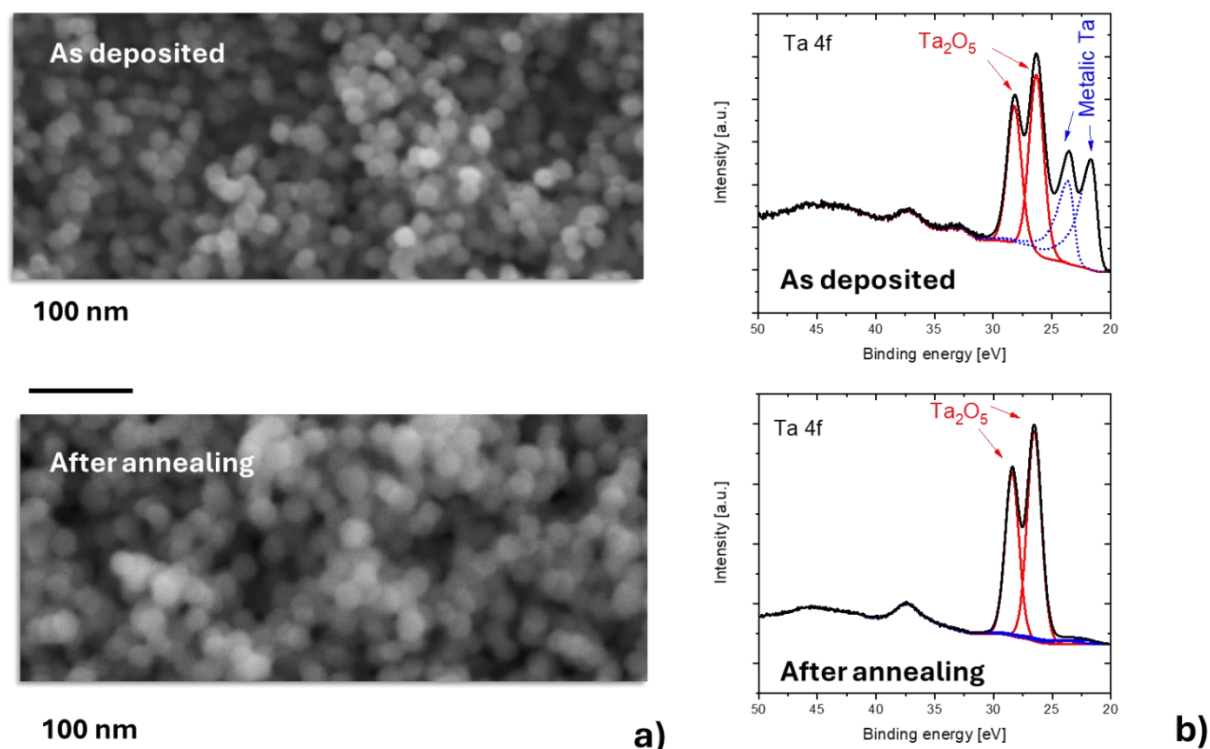


**Figure 2 a)** Top-view SEM images of deposited Ta NPs before (top) and after (bottom) annealing. **b)** High-resolution XPS spectra of Ta 4f peak of Ta NPs before (top) and after (bottom) annealing.

Subsequently, thermal annealing was performed to promote further Ta oxidation. As depicted in **Figure 2**, this annealing step resulted in a slight increase in the mean nanoparticle size to  $23 \pm 3$  nm, which is consistent

with oxygen incorporation and structural rearrangement. More importantly, the annealing led to the complete abatement of the metallic Ta<sup>0</sup> signal in the XPS spectra, confirming the near-complete oxidation of the NPs.

### 3.2 Ta<sub>2</sub>O<sub>5</sub>/Au bi-component coatings

In order to fabricate bi-component Ta<sub>2</sub>O<sub>5</sub>/Au nanoparticle-based coatings, 3 different strategies were followed. The first strategy involved the Au sputter-deposition onto a film composed of Ta<sub>2</sub>O<sub>5</sub> NPs. This approach, previously utilised for producing SERS-active V<sub>2</sub>O<sub>5</sub>/Au platform [4], relies on the Volmer-Weber growth mechanism [10]. A short deposition pulse (10 seconds) was used, resulting in the formation of isolated Au nano-islands randomly distributed across the exposed Ta<sub>2</sub>O<sub>5</sub> NPs surface (**Figure 3**). A principal benefit of this deposition procedure is the complete decoupling of the MeO nanoparticle synthesis from the subsequent metal deposition, which makes it applicable for the fabrication of systems composed of various TMeO/Me combinations. The primary constraint, however, is the spatial confinement of the metallic nanostructures exclusively to the topmost surface layer of the TMeO NPs film.

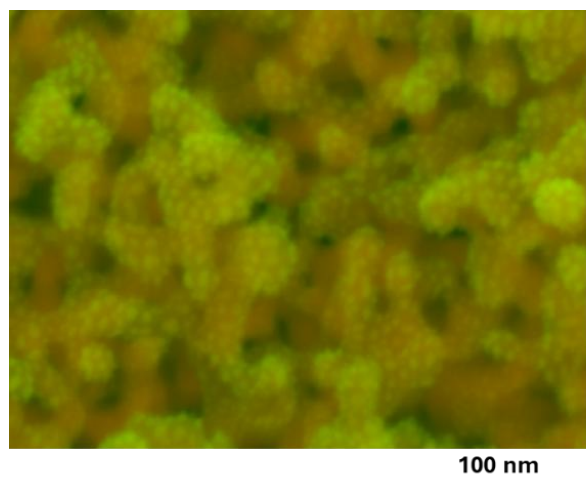


**Figure 3** Top-view of Ta<sub>2</sub>O<sub>5</sub>/Au nanoparticle-based coatings. False green colour corresponds to the SEM image acquired in SE mode, false red colour corresponds to the SEM image acquired in BSE mode.

To mitigate the limitation of surface confinement inherent in the aforementioned deposition procedure, the second strategy utilises a sequential, alternating deposition process. This approach leads to a multilayer sandwich heterostructure composed of alternating layers of Ta NPs and Au interlayers. **Figure 4a** illustrates a cross-section of a representative coating fabricated using 5 Ta NPs layers interspaced by 4 Au-containing interlayers. The individual Ta NPs layers were deposited for a fixed duration of 2 minutes, while the Au interlayers were formed by sputtering for 30 seconds in each cycle. The successful formation and periodicity of this layered architecture were further confirmed by EDS elemental mapping (**Figure 4b**). However, to obtain Ta<sub>2</sub>O<sub>5</sub>/Au heterostructure, the coatings have to be annealed. As shown in **Figure 4c** and **Figure 4d**, the layered structure is maintained even after 30 minutes of the thermal treatment at 500 °C, i.e., at the conditions that assure complete transformation of as-deposited Ta NPs into Ta<sub>2</sub>O<sub>5</sub> ones (see **Figure 2b**).

Complementing the sequential approach, the third strategy involves the simultaneous co-deposition of Ta NPs and Au. This technique allows for the variation of film composition, which is controlled by the relative fluxes of Ta NPs and sputtered Au atoms. Cross-sectional SEM images (**Figure 5a**) obtained from coatings fabricated under different Au magnetron currents illustrate the resulting architecture. These images, together with EDX analysis of the annealed films (**Figure 5b**), provide evidence that the Au nano-islands are homogeneously dispersed throughout the entire thickness of the coating. Furthermore, the number of incorporated Au nano-islands is directly controlled by adjusting the magnetron current applied to the Au sputtering source during the co-deposition process.

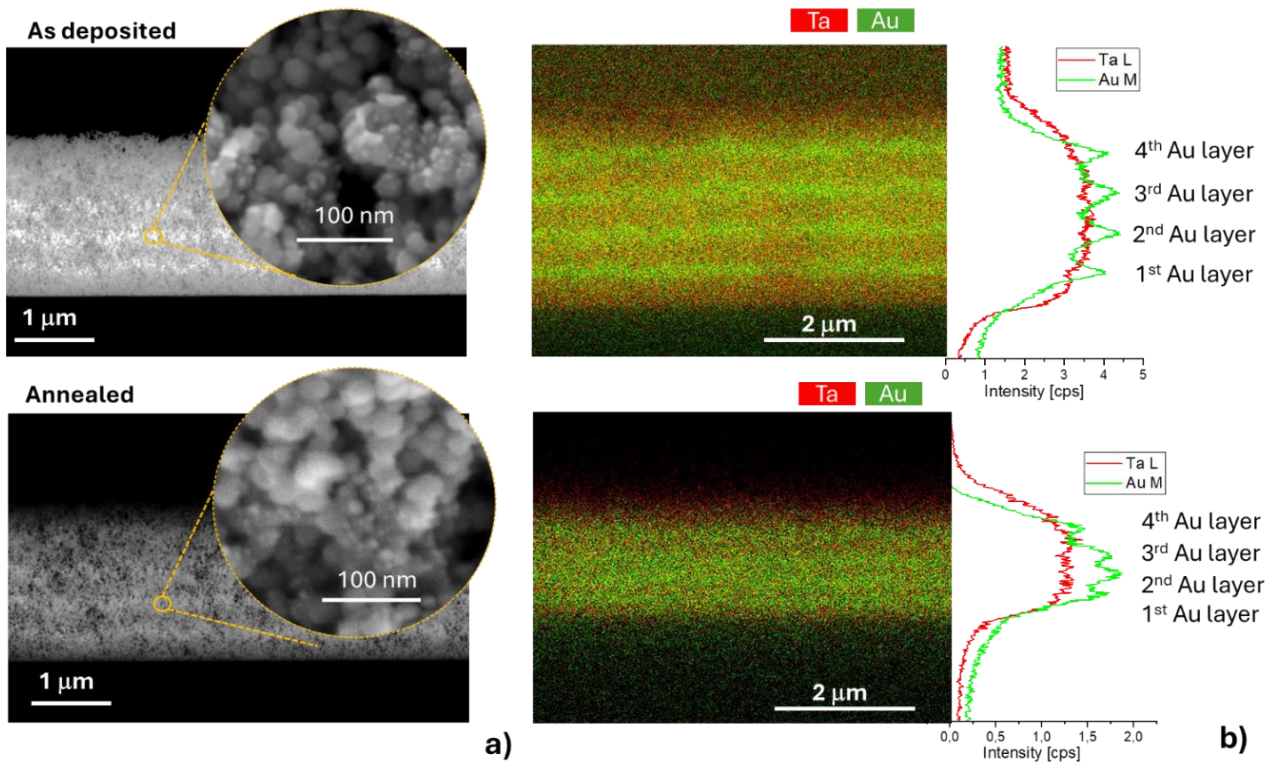


**Figure 4** a) Cross-section of SEM image of layered structure before (top) and after the thermal annealing measured in BSE mode, and details of Au-containing section of the coatings measured in SE mode. b) EDS mapping of Ta and Au elemental profile of as-deposited (top) and annealed (bottom) samples.

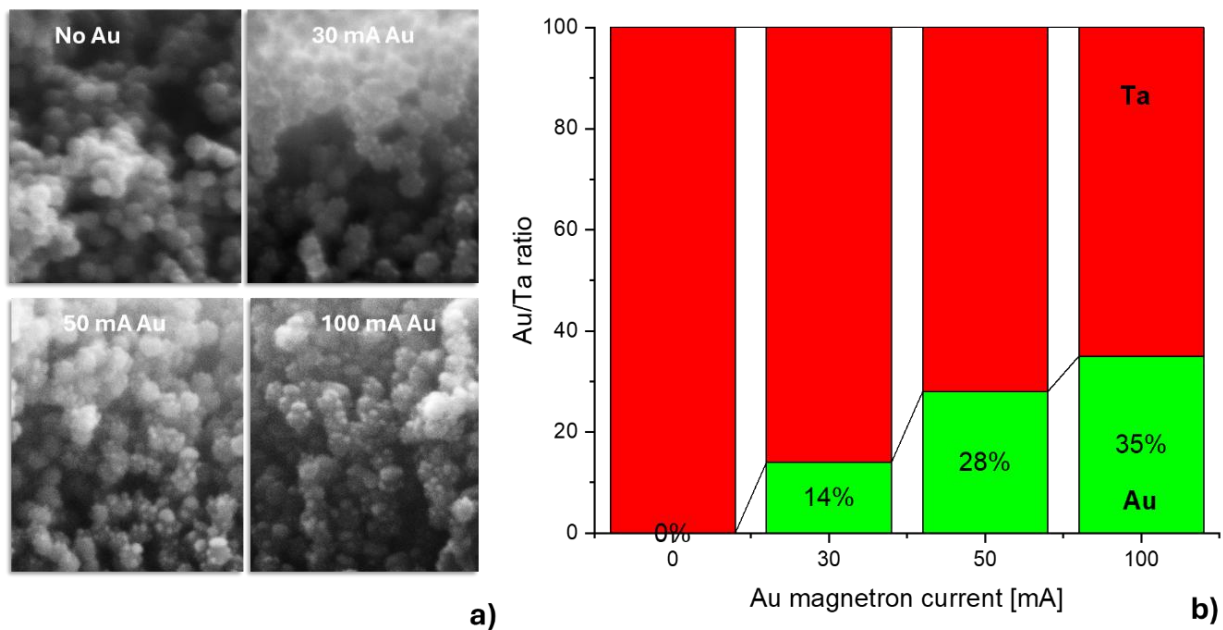


**Figure 5** a) SEM images of the cross-section of Ta<sub>2</sub>O<sub>5</sub>/Au nanoparticle-based coatings produced by simultaneous deposition of Ta NPs and Au at different magnetron currents used for Au sputtering. b) Au/Ta ratio as a function of Au magnetron current as determined by EDX.

#### 4. CONCLUSION

To conclude, this work successfully established three distinct strategies applicable for the fabrication of TMeO/Me porous nanoparticle-based coatings. These strategies included: (i) the surface decoration of TMeO nanoparticle films produced by gas aggregation source and oxidised by thermal annealing; (ii) the creation of multilayer heterostructures via the sequential, alternating deposition of transition metal nanoparticles and metallic nano-islands, followed by a thermal treatment; and (iii) the formation of a random nanocomposite structure via the simultaneous co-deposition of the transition metal nanoparticles and the metal component, also followed by thermal annealing. As demonstrated using the Ta<sub>2</sub>O<sub>5</sub>/Au system, these pathways enable the rational design of TMeO/Me coatings with tuneable architectures, i.e., a crucial step for designing next-generation functional nanomaterials. However, it is worth mentioning that while the strategy (i) is versatile in terms of materials used for TMeO/Me production, as the formation of TMeO NPs and deposition of metallic nano-islands are fully decoupled, a critical challenge associated with strategies (ii) and (iii) is the requirement for a final post-deposition thermal annealing step. This process sequence places an inherent constraint on the maximum achievable annealing temperature. Specifically, the annealing temperature must be kept relatively low, primarily dictated by the size-dependent thermal stability of metallic nano-islands. Consequently, this temperature limitation presents an obstacle for certain TMeO materials that may necessitate a higher annealing temperature to reach the desired oxidative state required for optimal device performance.

#### ACKNOWLEDGEMENTS

*This work was supported by the grant GAČR 25-14402L from the Czech Science Foundation.*

#### REFERENCES

- [1] KUMAR, S., LODHI, D.K., SINGH, J.P. Highly sensitive multifunctional recyclable Ag–TiO<sub>2</sub> nanorod SERS substrates for photocatalytic degradation and detection of dye molecules. *RSC Advances*. 2016, vol. 6 (2016), pp. 45120-45126.
- [2] FANG, H., ZHANG, C.X., LIU, L. et al. Recyclable three-dimensional Ag nanoparticle-decorated TiO<sub>2</sub> nanorod arrays for surface-enhanced Raman scattering. *Biosensors and Bioelectronics*. 2015, vol. 64, pp. 434-441.
- [3] XIE, Y., JIN, Y., ZHOU, Y., WANG, Y. SERS activity of self-cleaning silver/titania nanoarray. *Applied Surface Science*. 2014, vol. 313, pp. 549-557.
- [4] PROCHÁZKA, M., NOVÁK, D., KOČIŠOVÁ, E., KYLIÁN, O., OZAKI, Y. New Insights into SERS Mechanism of Semiconductor–Metal Heterostructure: A Case Study on Vanadium Pentoxide Nanoparticles Decorated with Gold. *Journal of Physical Chemistry C*. 2024, vol. 128, pp. 11732–11740.
- [5] BEN-JABER, S., PEVELER, W.J., QUESADA-CABRERA, R., et al. Photo-induced enhanced Raman spectroscopy for universal ultra-trace detection of explosives, pollutants and biomolecules. *Nature Communications*. 2016, vol. 7, p. 12189.
- [6] PIETA, L., KISIELEWSKA, A., Piwoński, I., MALEK, K. Modulation of photo-induced Raman enhancement in Ag nanoparticles deposited on nanometer-thick TiO<sub>2</sub> films. An interplay between plasmonic properties and irradiation energy. *Spectrochimica Acta Part A: Molecular and Biomolecular Spectroscopy*. 2024, vol. 305, 123537.
- [7] SHONDO, J., VEZIROGLU, S., TJARDTS, T., et al. Nanoscale synergetic effects on Ag–TiO<sub>2</sub> hybrid substrate for photoinduced enhanced Raman spectroscopy (PIERS) with ultra-sensitivity and reusability. *Small*. 2022. vol. 18, 2203861.
- [8] HABERLAND, H., KARRAIS, M., MALL, M., THURNER, Y. Thin films from energetic cluster impact: a feasibility study, *Journal of Vacuum Science and Technology A*. 1992, vol. 10, pp. 3266–3271.
- [9] ATANASSOVA, E., SPASSOV, D. X-ray photoelectron spectroscopy of thermal thin Ta<sub>2</sub>O<sub>5</sub> films on Si. *Applied Surface Science*. 1998, vol. 135, pp. 71-82.
- [10] OHRING, M. *The Materials Science of Thin Films*, New York: Academic Press, 1992.